JOC The Journal of Organic Chemistry

ARTICLE

pubs.acs.org/joc

Evidence for the Role of Tetramethylethylenediamine in Aqueous Negishi Cross-Coupling: Synthesis of Nonproteinogenic Phenylalanine Derivatives on Water

Andrew J. Ross,[†] Frank Dreiocker,[‡] Mathias Schäfer,[‡] Jos Oomens,[§,∥] Anthony J. H. M. Meijer,[†] Barry T. Pickup,[†] and Richard F. W. Jackson*[,†]

[†]Department of Chemistry, The University of Sheffield, Dainton Building, Sheffield, S3 7HF, U.K.

[‡]Department of Chemistry, University of Cologne, Greinstrasse 4, 50939 Köln, Germany

[§]FOM Institute for Plasma Physics Rijnhuizen, Edisonbaan 14, Nieuwegein 3439 MN, The Netherlands

[∥]University of Amsterdam, Science Park 904, 1098XH Amsterdam, The Netherlands

Supporting Information

ABSTRACT: The structure of the alkylzinc−tetramethylethylenediamine (TMEDA) cluster cation **3** has been determined in the gas phase by a combination of tandem mass spectrometry, infrared multiphoton dissociation (IRMPD) spectroscopy, and DFT calculations. Both sets of experimental results establish the existence of a strongly stabilizing interaction of TMEDA with the zinc cation. High-level DFT calculations on the alkylzinc−TMEDA cluster cation **3** allowed the identification of two low energy conformers, each featuring a four-coordinate zinc atom with a bidentate TMEDA ligand, and internal coordination from the carbonyl group of the Boc group to zinc. The experimental IRMPD spectrum is reproduced with an appropriately weighted combination of the IR spectra of the two conformers identified by theory. DFT calculations on the structure of the alkylzinc halide **2** with coordinated TMEDA using the PCM model of water solvent suggest that TMEDA can promote ionization of the zinc−iodine bond in organozinc iodides under aqueous conditions, providing a credible explanation for the role of TMEDA in stabilizing the carbon−zinc bond. Reaction of the serine-derived iodide **1** with aryl iodides "on water", promoted by nano zinc in the presence of $PdCl_2(Amphos)_2$ (5 mol %) and TMEDA, leads to the formation of protected phenylalanine derivatives **4** in reasonable yields. In the case of ortho-substituted aryl iodides and aryl iodides that are solids at room temperature, conducting the reaction at 65 °C gives improved results. In all cases, the product **5** of reductive dimerization of the iodide **1** is also isolated.

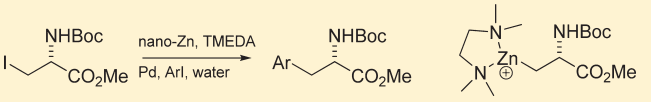

INTRODUCTION

We have recently structurally characterized a series of functionalized alkylzinc cations in the gas phase[1] by use of electrospray ionization and IRMPD spectroscopy.[2,3] Related studies on solvated alkylzinc cations[4] and on organozincates[5,6] using ESI have been reported by Koszinowski, and other studies exploring the correlation between ESI spectra of metal/ligand complexes and their solution properties have been reviewed.[7] The functionalized alkylzinc cations that we studied were obtained from the corresponding alkylzinc iodides prepared in DMF solution and contain coordinated DMF solvent. DFT calculations have suggested that coordination of DMF to alkylzinc iodides can induce (partial) cleavage of the zinc−iodine bond to form a tight ion pair,[8] resulting in significant cationic character at zinc. An expected consequence is that the resulting alkylzinc cation is much less easy to protonate than a neutral alkylzinc iodide, providing a credible explanation for the high tolerance of alkylzinc iodides toward acidic protons. Recently, Lipshutz has reported that treatment of simple alkyl iodides with zinc, aryl bromides, a nonionic surfactant, a palladium catalyst, and crucially TMEDA, in water, leads to the products of Negishi cross-coupling.[9] When benzylic halides were used as substrates under similar conditions (although in the absence of a surfactant), the products of cross-coupling were obtained in an "on-water" reaction.[10] Lipshutz suggested that TMEDA, a strongly coordinating ligand, might play a role in stabilizing the presumed alkylzinc halide intermediates in the presence of water.[10,11] It appeared to us that the mechanism of such stabilization might involve TMEDA-induced ionization of the zinc−halogen bond, as we had previously suggested with DMF as ligand,[8] as shown in eq 1. TMEDA adducts of alkylzinc cations have been detected in the gas phase,[4] suggesting that this process can occur.

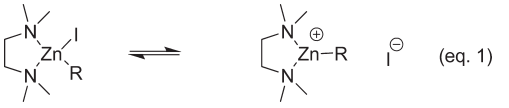

Furthermore, the possibility of applying the Lipshutz conditions to the alkyl iodide **1**, which has been widely employed for

Received: December 1, 2010
Published: February 14, 2011

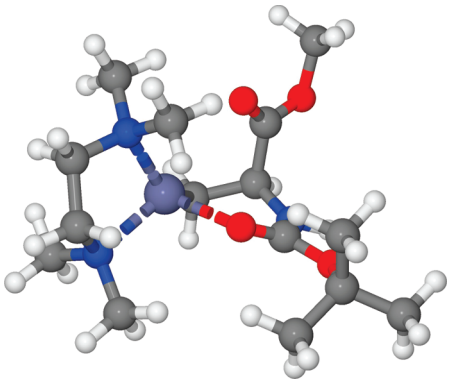

Figure 1. Calculated structure of cation **3** (axial methyl ester) in the gas phase.

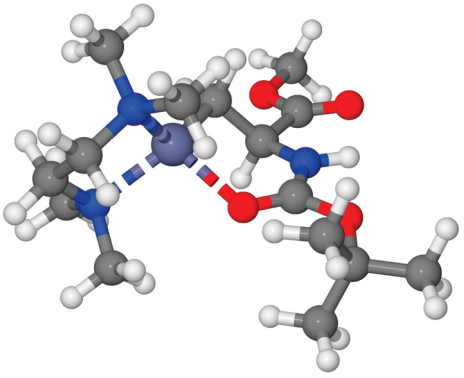

Figure 2. Calculated structure of cation **3** (equatorial methyl ester) in the gas phase.

the synthesis of enantiomerically pure α-amino acids,[12,13] appeared to be very attractive, since it potentially opens the possibility of applying Negishi cross-coupling to post-translational modification of peptides in the presence of water.[14] The compatibility of iodide precursor **1** with TMEDA remained to be established, since the iodide **1** is known to be sensitive to base, undergoing elimination to the corresponding dehydroalanine derivative.

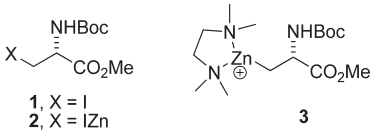

RESULTS AND DISCUSSION

While structure determination in solution is complex due to solvation and conformational mobility, we have already established that a combination of IRMPD and DFT calculations can be used for precise structure determination of alkylzinc cations in the gas phase.[1] As a starting point, we have therefore investigated the structure of zinc cations derived from alkylzinc iodide **2**, with coordinated TMEDA. Calculations on the free cation **3** allowed the identification of two low energy conformers, featuring four-coordinate zinc, with a bidentate TMEDA ligand and internal coordination from the carbonyl group of the Boc group to zinc.

Scheme 1. Fragmentation Reactions of the Alkylzinc−TMEDA Cluster Ion 3 at *m/z* 382 upon CID in an Octapole[a]

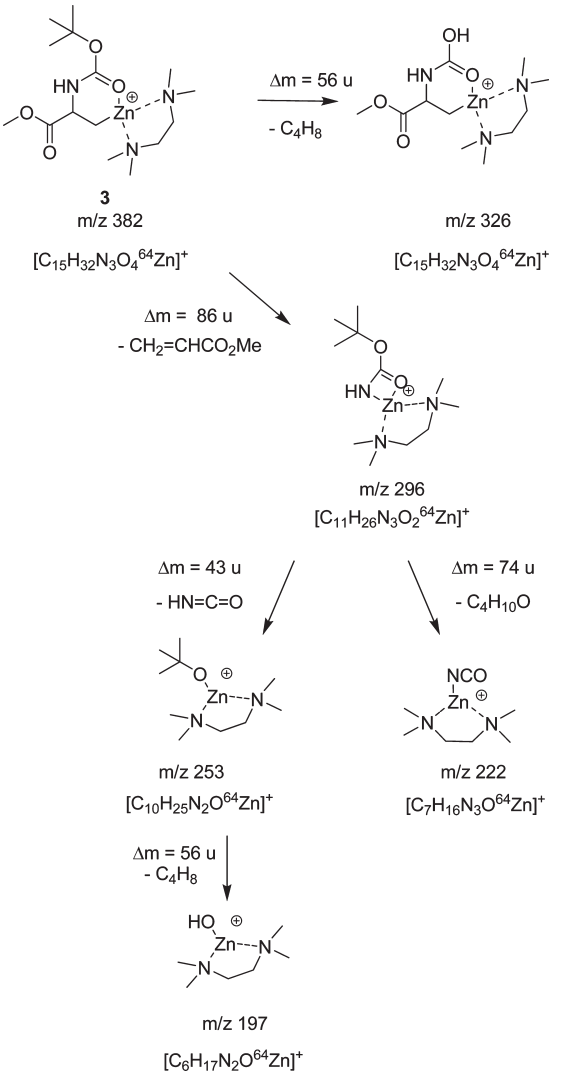

[a] The depicted ion structures are indicative and are consistent with determined accurate ion masses.

These calculations suggested that, in vacuo, the conformer with the axial methyl ester (Figure 1) was more stable than the conformer with an equatorial methyl ester (Figure 2), which was found to be 5.9 kJ mol^{-1} higher in energy. The calculations were conducted with BSSE corrections,[15] although the stability order was not influenced by such corrections. It appears that the ester carbonyl in the axial conformation can interact with the cationic zinc center, and this evidently provides more stabilization than the alignment of the carbamate N−H and the ester carbonyl through minimization of the dipole.[1]

In order to explore the structure experimentally, the alkylzinc iodide **2** was prepared from protected iodoalanine **1** in DMF, TMEDA added, and the solution studied by ESI-MS in positive-ion mode. The base peak in the ESI-MS spectrum exhibits the fingerprint isotopic pattern of zinc (see Figure 1S in the Supporting Information), and the ion at *m/z* 382 was identified to be the signal of the TMEDA cation **3**, by determination of the exact ion mass (^{64}Zn isotope). Due to the stability of ion **3** at *m/z* 382, it could easily be selected as a precursor for CID product ion

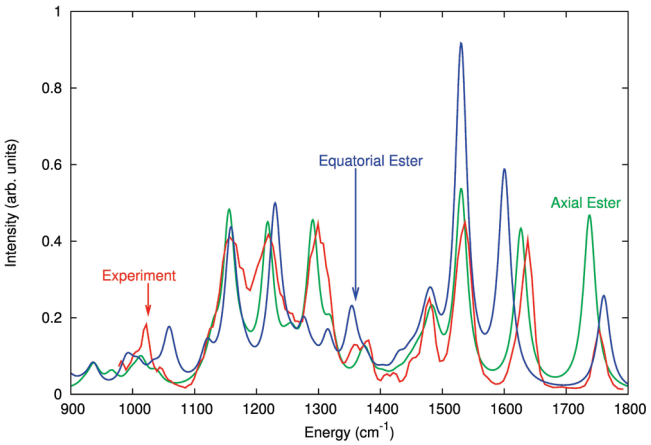

Figure 3. Comparison of experimental and calculated spectra (axial/equatorial) for cation **3**.

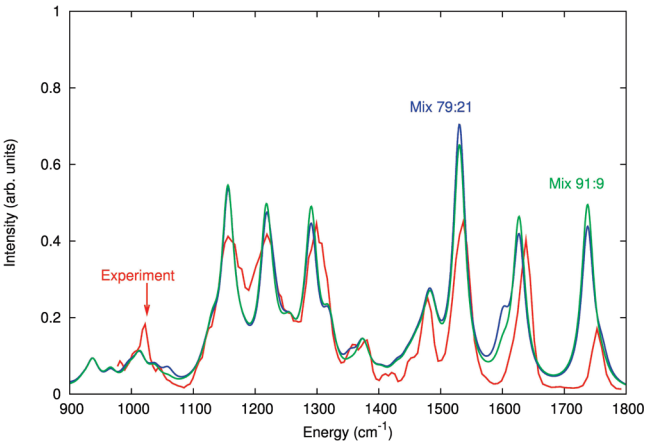

Figure 4. Comparison of experimental spectra (red) for cation **3** with the calculated spectrum resulting from a mixture of axial and equatorial methyl esters in ratios of 91:9 (green) and 79:21 (blue).

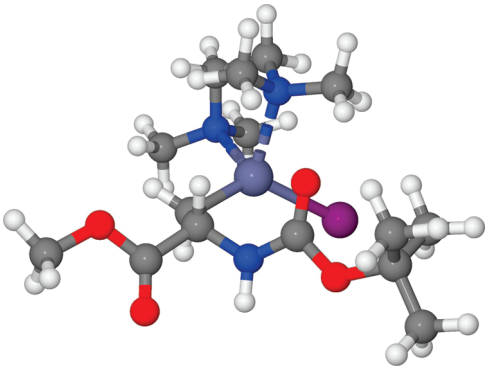

Figure 5. Calculated lowest energy structure for **2**. TMEDA in vacuo.

experiments which exhibit a number of characteristic fragment ions (Scheme 1). As Scheme 1 illustrates, the TMEDA ligand is retained throughout the activation events while parts of the organic ligand (e.g., 2-methylpropene, C_4H_8, and isocyanic acid HNCO) are lost in fragmentation reactions by rearrangement and cleavage of covalent bonds. This observation suggests the existence of a very strong interaction of the TMEDA ligand with the zinc ion, an interaction which apparently survives substantial activation. However, two product ions are found in the low mass range at m/z 70 and 115, which originate from secondary fragmentation reactions of the TMEDA−zinc precursor ions in the octapole CID product ion spectrum.

The TMEDA cation **3** was also sufficiently stable for IRMPD experiments.[1] Figure 3 shows the experimental spectrum, together with the theoretical spectra predicted for the axial and equatorial isomers. For comparison to IRMPD spectra, the experimental frequencies were scaled[16,17] by 0.98.[18,19] The intensities of both theoretical spectra were scaled (by the same amount) to obtain qualitative agreement between the theoretical spectra and the experimental spectrum for the peaks at between 1100 and 1300 cm^{-1}. As is clear from Figure 3, the agreement between the spectrum for the isomer with the axial methyl ester (Figure 1) and the experimental spectrum is almost exact. All major peaks coincide at approximately the right intensities, apart from the ester carbonyl stretch at 1750 cm^{-1}, the intensity of which was also overestimated in our earlier calculations.[1] The agreement between the spectrum for the isomer with the equatorial methyl ester (Figure 2) and the experimental data is less convincing. In particular, there are major discrepancies in the region between 1600 and 1800 cm^{-1} as well as a missing peak at 1300 cm^{-1} and a spurious one at 1075 cm^{-1}. As a result we can conclude with confidence that the major isomer of cation **3** observed in the experiment has the methyl ester in an axial orientation (Figure 1). It is necessary to express the caveat that all our calculations are done in the harmonic approximation and assume linear absorption conditions, whereas IRMPD spectroscopy involves a multiphoton nonlinear process in which intensities and band widths are influenced in a subtle manner by the extent of anharmonicity of the vibrations and by unpredictable coupling of vibrational modes.[20,21] However, it has been established that relative intensities of IRMPD spectra are in fair agreement with those of linear absorption spectra,[3,22,23] which makes us confident of our assignment.

However, from the energy difference between isomers (5.9 kJ/mol) it is clear that we should consider the possibility that more than one isomer is present. To investigate this further we simulated two additional spectra, based on mixtures of axial and equatorial isomers. The composition of these mixtures was taken from either the energy difference between the isomers (leading to a 91:9 mixture in favor of the axial isomer) or the Gibbs energy difference (3.3 kJ mol^{-1}) between the isomers (leading to a 79:21 mixture in favor of the axial isomer). These spectra are plotted in Figure 4 with the experimental spectrum. When these spectra are compared to the pure spectrum for the axial isomer in Figure 3, it is clear that each of the simulated spectra in Figure 4 give an agreement with the experimental spectrum that is as good as the agreement for the axial isomer, meaning that indeed we cannot exclude the possibility of two isomers being present.

Having determined the structure of the cation **3** in the gas phase, which demonstrated the effectiveness of DFT methods for determining the structures of relevant species (at least in vacuo), attention now turned to the more complex problem of investigating the structure of the alkylzinc halide **2** with coordinated TMEDA. Two sets of DFT calculations[24] were therefore conducted to determine the structure of the alkylzinc iodide **2** with coordinated TMEDA. The first set of calculations was carried out

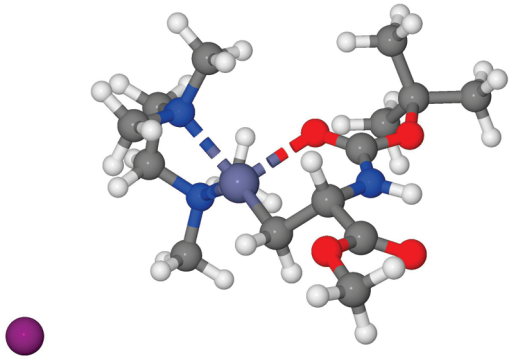

Figure 6. Calculated lowest energy structure for **2**·TMEDA in water using PCM.

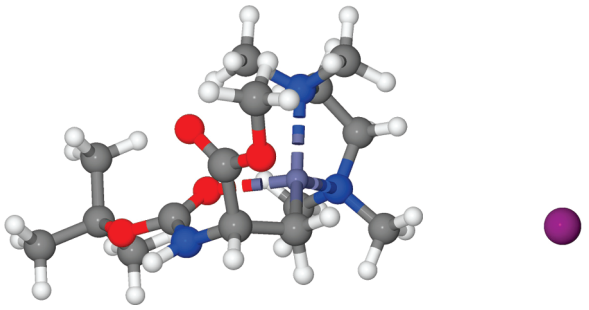

Figure 7. Calculated structure for **2**·TMEDA with an axial ester in water using PCM.

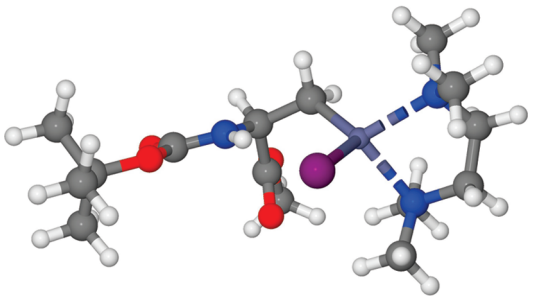

Figure 8. Calculated lowest energy covalent structure for **2**·TMEDA in water using PCM.

in vacuo, as this more closely resembles the situation already studied experimentally. The second set of calculations was conducted with a PCM model of water solvent. The latter calculations were designed to allow an investigation of the structure of the alkylzinc iodide **2** with coordinated TMEDA in an aqueous environment, as a prelude to applying the Lipshutz conditions to iodide **1**. We note that these calculations were not subjected to BSSE corrections, since they are unavailable for PCM.

All the low energy conformations that were identified in vacuo for the structure of the alkylzinc halide **2** with coordinated TMEDA feature a four-coordinate zinc atom with a bidentate TMEDA ligand and an intact zinc−iodine bond. The lowest energy conformer identified is shown in Figure 5. The carbamate N−H and the ester carbonyl are aligned, so as to minimize the dipole (as we have seen before).[8]

Scheme 2. Preparation of Phenylalanine Derivatives 4 Using Liquid Aryl Iodides

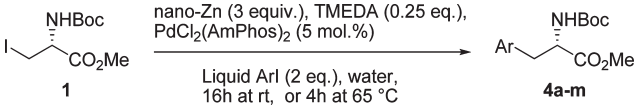

Table 1. Preparation of Phenylalanine Derivatives 4 Using Liquid Aryl Iodides

			yield (%)	
entry	Ar	product	room temp	65 °C
1	C_6H_5	**4a**	67 (66)[a]	
2	C_6H_5	**4a**	35[b]	
3	$C_{10}H_7$	**4b**	24	29
4	2-MeC_6H_4	**4c**	20	19
5	2-FC_6H_4	**4d**	18	37
6	2-ClC_6H_4	**4e**	17	32
7	3-$MeOC_6H_4$	**4f**	51	56
8	3-$CF_3C_6H_4$	**4g**	47	48
9	3-ClC_6H_4	**4h**	44	54
10	3,5-$F_2C_6H_3$	**4i**	39	54
11	4-FC_6H_4	**4j**	50	72
12	4-FC_6H_4	**4j**	34[b]	
13	4-$CF_3C_6H_4$	**4k**	42	42
14	3,4-$F_2C_6H_3$	**4l**	51	53

[a] Using $PdCl_2(Amphos)_2$ (1 mol %). [b] Using the corresponding aryl bromide.

However, when calculations were carried out using a PCM model of water solvent, the lowest energy structure identified now featured internal coordination of the carbamate carbonyl group to zinc, an equatorial ester group, and ionization of the zinc−iodine bond (Figure 6). The conformer with an axial ester (Figure 7) was higher in energy by 3.5 kJ mol^{-1}, and the lowest energy covalent conformer (Figure 8) was less stable again by a further 1.9 kJ mol^{-1}. Notwithstanding the fact that PCM only takes into account the interaction of a molecule with a bulk dielectric medium and that hydrogen bonding is not included, these results suggest that the ionization shown in eq 1 can indeed occur under aqueous conditions and encouraged us to explore possible synthetic applications of the alkylzinc iodide **2** under aqueous conditions.

Phenylalanine Synthesis in Water. Initial application of the Lipshutz "in water" conditions[9] to protected iodoalanine **1** and iodobenzene, at room temperature, in the presence of a variety of surfactants (Tween 80, PTS and Brij 30, as 2% solutions in water), was encouraging in that protected phenylalanine **4a** was formed, but the yields were low (6−27%) and substantial amounts of the starting iodide **1** were isolated. Reactions carried out in the absence of surfactant, the "on water" conditions,[10] gave a similarly low yield of **4a** (16%). Although Lipshutz has reported that the use of nano zinc with less functionalized alkyl halides resulted in an uncontrolled reaction, and led only to protonation of the organozinc reagent,[11] use of nano zinc in place of zinc dust with the iodide **1** gave much improved results. Optimized reaction conditions used $PdCl_2(Amphos)_2$ (5 mol %), nano zinc

Table 2. Optimization of the Cross-Coupling Reaction of 1 with 4-Chloroiodobenzene

entry	temp (°C)	cosolvent	time (h)	yield of **4n** (%)
1	20		16	16
2	20	THF	16	43
3	20	toluene	16	40
4	65		3	36
5	65		4	64 (73)[a]
6	65	THF	4	37
7	65	toluene	4	42

[a] 2 equiv of 4-chloroiodobenzene used.

Scheme 3. Negishi Cross-Coupling with Solid Aryl Iodides

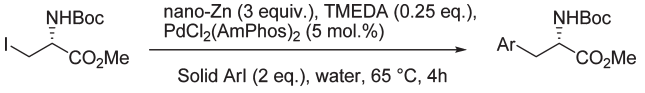

1 **4n-r**

Table 3. Negishi Cross-Coupling with Solid Aryl Iodides at 65 °C

entry	Ar	ArI mp (°C)	product	yield (%)
1	4-ClC_6H_4	53−54	**4n**	73 (32)[a]
2	3-HOC_6H_4	42−44	**4o**	28
3	4-MeC_6H_4	33−35	**4p**	62
4	4-HOC_6H_4	92−94[b]	**4q**	35
5	4-$MeOC_6H_4$	50−52	**4r**	51

[a] Using $PdCl_2(Amphos)_2$ (1%). [b] When this reaction was conducted at 95 °C, only decomposition products were observed.

(3 equiv), aryl iodide (2 equiv), and TMEDA (0.25 equiv), as had already been established by Lipshutz,[10] allowed protected phenylalanine **4a** to be obtained in much improved yield (67%, based on protected iodoalanine **1**) (Scheme 2).

Exemplification of the optimized conditions for coupling with liquid aryl iodides was then undertaken (Scheme 2, Table 1). Ortho-substituted aryl iodides give poor yields, while other substrates give moderate yields. This behavior is reminiscent of the results obtained using our original method for making phenylalanine derivatives using $Pd_2dba_3/(o\text{-tol})_3P$ in THF as solvent.[25] When the coupling reactions were conducted at 65 °C, significant improvements in yields were obtained using some ortho-substituted aryl iodides (Table 1, entries 5 and 6) and also with several other cases (Table 1, entries 9−11). The conditions have not been individually optimized for each substrate. In favorable cases, the palladium loading can be reduced to 1 mol % without the yield decreasing significantly (Table 1, entry 1). Two aryl bromides were investigated and gave substantially lower yields than the corresponding aryl iodides (Table 1, entries 2 and 12).

Application of the room temperature conditions to 4-chloroiodobenzene gave a very disappointing yield of the desired product **4n** (16%) that was significantly lower than expected based on our previous assessment of the relative reactivity of iodobenzene and 4-chloroiodobenzene.[13] The only significant difference is the physical state of the electrophile (iodobenzene is

Scheme 4. Reductive Dimerization of Protected Iodoalanine 1

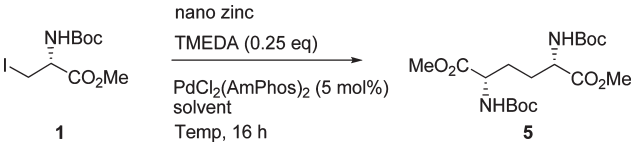

1 **5**

Table 4. Reductive Dimerization of Protected Iodoalanine 1

entry	solvent	temp (°C)	yield (%)
1	H_2O/toluene	20	8
2	H_2O/toluene	65	40
3	DMF	20	38
4	DMF	65	44
5[a]	DMF	65	21

[a] No $PdCl_2(Amphos)_2$ used.

a liquid and 4-chloroiodobenzene is a solid, mp 53−54 °C). A series of optimization experiments was carried out to investigate the role of temperature, cosolvent, and the influence of the amount of aryl iodide on the efficiency of the cross-coupling (Table 2). As is evident, better results were obtained when the reaction was conducted at 65 °C (Table 2, entry 5), and somewhat surprisingly in the absence of added cosolvent (Table 2, cf. entry 5 with entries 6 and 7). The optimum yield was obtained using a 2-fold excess of the aryl iodide, resulting in a much improved yield of the desired product **4n** (73%). Attempts were made to undertake the reaction in the absence of water, but the melt was too viscous to stir effectively. From these results it appears likely that the reaction is taking place on the surface of the water ("on water"[10]) and that for best results the aryl iodide needs to be liquid at the temperature at which the reaction is conducted.

Application of the modified method to a range of solid aryl iodides was then undertaken. For (relatively) low-melting aryl iodides, the general method works reasonably effectively (Scheme 3, Table 3). Use of lower catalyst loadings resulted in a pronounced reduction in yield (Table 3, entry 1). Although the yields for iodophenols (Table 3, entries 2 and 4) are low, it is encouraging that the reaction works at all given the enhanced acidity of phenols in water, compared to the situation in a dipolar aprotic solvent,[26] in which we had done all our previous Negishi cross-coupling reactions with iodophenols.[13,27] The ortho-substituted solid aryl iodides that we employed (2-OH and 2-NH_2) gave only trace amounts of product, probably due to a combination of slower Negishi cross-coupling and enhanced ease of protonation of the organozinc reagent.

In all of the examples we have undertaken in aqueous conditions, the homocoupled product **5** is recovered in variable yields depending on the aromatic halide used. When protected iodoalanine **1** was subjected to the cross-coupling conditions, but in the absence of electrophile, none of the homocoupled product **5** was formed and iodoalanine **1** was recovered. However, addition of toluene as a cosolvent and warming to 65 °C now allowed a significant amount of the homocoupled product **5** to be isolated (Table 4, cf. entries 1 and 2) (Scheme 4). Similar results could be obtained under nonaqueous conditions using DMF as

dx.doi.org/10.1021/jo102334c |J. Org. Chem. 2011, 76, 1727–1734

solvent, although warming was now less critical (Table 4, cf. entries 3 and 4). Interestingly, homocoupling was also observed in the absence of palladium (Table 4, entry 5) in a reaction that is the zinc analogue of the Wurtz coupling. In all cases, the mass balance is protected alanine, arising from protonation of the zinc reagent **2**. Interestingly, treatment of the organozinc reagent **2** in DMF with iodide **1** in the presence of $PdCl_2(Amphos)_2$ gave none of the expected product **5**, from which we can conclude that a simple sp^3-sp^3 Negishi cross coupling is not taking place. Whatever the mechanism, reductive dimerization of iodoalanine with nano zinc in the presence of TMEDA does provide a simple method for the formation of the protected bis-amino acid **5**.

CONCLUSIONS

In conclusion, we have presented evidence that TMEDA stabilizes alkylzinc iodides toward protonation in the presence of water by inducing ionization of the zinc−iodine bond and have structurally characterized the cation potentially derived from such ionization in the gas phase. We have also shown that phenylalanine derivatives can be synthesized using Negishi cross-coupling in the presence of water, without preformation of the organozinc reagent. A range of substituents is tolerated by these conditions, which promise to be useful for the post-translational modification of peptides in the presence of water.

EXPERIMENTAL SECTION

Materials. The alkylzinc reagent **2** was prepared as previously reported[1] as a solution in dry dimethylformamide.

Mass Spectrometry. The TMEDA cation **3** is found in the gas phase after phase transfer with ESI. For the ESI-MS and tandem MS experiments, aliquots of the alkylzinc iodide solution of **2** were diluted with dry DMF to sub-millimolar concentrations. For the generation of TMEDA cation **3**, 10 μL of TMEDA was added to 1 mL of the DMF solution of **2**, and this mixture was subjected to ESI after stirring. Collision-induced dissociation (CID) experiments were performed on a Finnigan MAT 900 instrument with an EB-QIT configuration (ThermoFisher, Bremen, Germany) and have been described in detail elsewhere.[1] Exact ion mass measurements were conducted (external calibration; resolution >20000 fwhm) on a LTQ-Orbitrap instrument (ThermoFisher) equipped with an ESI ion source. All exact ion masses were determined with an experimental error ≤3 ppm.[1]

Infrared Multiphoton Dissociation Spectroscopy. A 4.7 T Fourier-transform ion cyclotron resonance (FTICR) mass spectrometer was used for the IRMPD experiments and has been described in detail elsewhere.[1,28−30]

The fragmentation reactions found in IRMPD of the TMEDA cation **3** were analogous to those found upon low energy CID (see Scheme 1). The IRMPD spectra were recorded by monitoring the most abundant product ions and the depletion of the respective precursor ion over the 900−1800 cm^{-1} range. The IRMPD yield was determined from the precursor (I_P) intensity and the intensity of the product ions ($\Sigma I_{\text{product ions}}$) after laser irradiation at each frequency:

$$\text{IRMPD yield} = \Sigma I_{\text{product ions}}/(I_P + \Sigma I_{\text{product ions}}) \quad (1)$$

The yield was normalized linearly with laser power to take account of the change in laser power as a function of photon energy.[20]

Computational Methods. All electronic structure calculations were carried out with the Gaussian 09 program package[24] using the B3LYP density functional.[31] The Dresden−Stuttgart pseudopotential[32,33] was used on Zn and I, and the basis set for all other atoms was at the 6-311G** level. Only electronic energies are reported. Gibbs energies are not generally reported because the existence of many extremely nonharmonic low-frequency modes for these flexible molecules renders the theoretical thermodynamic data unreliable. The low energy conformations of the unsolvated alkylzinc iodide are known from earlier work.[1] A series of TMEDA-solvated conformers was generated from each unsolvated conformer by placing TMEDA in all feasible positions and orientations around the zinc center. These candidate conformations were submitted to Gaussian for geometry optimization. The structures reported in this paper are derived from the resulting low energy local minima.

Two series of computations were performed. The first set (cf. Figures 1 and 2) on cationic species in vacuo were corrected for basis set superposition error (BSSE) using the Boys and Bernardi scheme.[15] BSSE corrections did not alter the energy order of the local energy minima we obtained but did affect the relative energies slightly. The resulting converged local geometries were used to obtain harmonic frequencies with BSSE corrections. The overestimation of these frequencies was corrected using the standard scaling approach[16,17] with a scaling factor of 0.98. Spectra were generated with in-house software by using calculated IR intensities broadened by a Lorentzian of width 15 cm^{-1}. These spectra were compared to the experimental IRMPD spectra in order to make a structural assignment. The second set of calculations was carried out on the neutral alkylzinc iodides with coordinated TMEDA without BSSE corrections. The calculation reported in Figure 5 was carried out in vacuo, while the remaining calculations (Figures 6−8) use the polarizable continuum model (PCM)[34] to represent the effects of water solvent (ε = 78.3553) using the integral equation formalism variant (IEFPCM).

General Cross-Coupling: Method A. Nano zinc dust (190 mg, 3 mmol) was added to a nitrogen-purged round-bottom flask followed by $PdCl_2(AmPhos)_2$ (35 mg, 0.025 mmol). Water (1 mL) was added via syringe under nitrogen, followed by tetramethylethylenediamine (23 μL, 0.25 mmol). Aryl iodide (2 mmol) followed by protected iodoalanine **1** (329 mg, 1 mmol) were then added with vigorous stirring. The reaction was allowed to stir at room temperature overnight under positive pressure of nitrogen. The crude reaction mixture was applied directly to a silica gel column to afford the purified cross-coupled product.

General Cross-Coupling: Method B. Nano zinc dust (190 mg, 3 mmol) was added to a nitrogen-purged round-bottom flask followed by $PdCl_2(AmPhos)_2$ (35 mg, 0.025 mmol). Water (1 mL) was added via syringe under nitrogen, followed by tetramethylethylenediamine (TMEDA, 23 μL, 0.25 mmol). The aryl iodide (2 mmol) and protected iodoalanine **1** (329 mg, 1 mmol) were then added with vigorous stirring. The reaction was heated to 65 °C and stirred for 4 h under positive pressure of nitrogen. The crude reaction mixture was applied directly to a silica gel column to afford the purified cross-coupled product.

(*S*)-Methyl 2-(*tert*-Butoxycarbonylamino)-3-(3-(trifluoromethyl)phenyl)propanoate, 4g. Following general cross-coupling, method A using 3-iodobenzotrifluoride (288 μL, 2 mmol) gave, after purification by silica gel column (5% EtOAc in toluene), **4g** (164 mg, 47%) as a red/brown oil, which solidified on standing. Method B gave **4g** (165 mg, 48%): mp 62−64 °C; R_f 0.67 (30% EtOAc in toluene); IR ν_{max}(film)/cm^{-1} 2978, 1743, 1702, 1500, 1451, 1367, 1326; NMR δ_H (400 MHz, $CDCl_3$) 1.43 (9H, s), 3.11 (1H, dd, J = 13.8, 6.1 Hz), 3.24 (1H, dd, J = 13.8, 5.6 Hz), 3.74 (3H, s), 4.63 (1H, dd, J = 13.8, 6.1 Hz), 5.07 (1H, d, J = 7.4), 7.33−7.40 (2H, m), 7.44 (1H, t, J = 7.7 Hz), 7.53 (1H, d, J = 7.6 Hz); δ_C (101 MHz, $CDCl_3$) 28.2, 38.2, 52.3, 54.3, 80.1, 123.9 (q, J = 3 Hz), 126.2, 128.9, 132.7, 137.2, 154.9, 171.9, two quaternary carbon signals not observed; $[\alpha]^{22}_D$ +30.8 (c 1.04, $CHCl_3$); MS m/z (ES) found 348.1433, $C_{16}H_{21}NO_4F_3$ requires MH^+ 348.1423.

(*S*)-Methyl 2-(*tert*-Butoxycarbonylamino)-3-(3-chlorophenyl)propanoate, 4h. Following general cross-coupling, method A using 1-iodo-3-chlorobenzene (247 μL, 2 mmol) gave, after purification

by silica gel column (3% EtOAc in toluene), **4h** (139 mg, 44%) as a red/brown oil. Method B gave **4h** (170 mg, 54%): R_f 0.57 (30% EtOAc in toluene); IR ν_{max}(film)/cm^{-1} 2978, 2927, 1743, 1711, 1502, 1478, 1436, 1366; NMR δ_H (400 MHz, $CDCl_3$) 1.42 (9H, s), 3.00 (1H, dd, J = 13.9, 6.0 Hz), 3.12 (1H, dd, J = 13.9, 5.6 Hz), 3.73 (3H, s), 4.57 (1H, dd, J = 13.9, 6.0 Hz), 5.00 (1H, d, J = 7.3 Hz), 6.98−7.03 (1H, m), 7.11 (1H, s), 7.22 (2H, d, J = 5.0 Hz); NMR δ_C (101 MHz, $CDCl_3$) 28.3, 38.1, 52.3, 54.3, 80.1, 127.2, 127.5, 129.5, 129.8, 134.3, 138.2, 172.0, one quaternary carbon not observed; $[\alpha]^{22}_D$ 59.4 (c 1.01, $CHCl_3$); MS m/z (ES) found 314.1171, $C_{15}H_{21}NO_4Cl$ requires MH^+ 314.1159.

(*S*)-Methyl 2-(*tert*-Butoxycarbonylamino)-3-(3,5-difluorophenyl)propanoate, 4i. Following general cross-coupling, method A using 3,5-difluoroiodobenzene (240 μL, 2 mmol) gave, after purification by silica gel column (5% EtOAc in toluene) **4i** (129 mg, 41%) as a red/pink solid. Method B gave **4i** (170 mg, 54%): mp 78−80 °C; R_f 0.63 (30% EtOAc in toluene); IR ν_{max}(film)/cm^{-1} 2980, 1743, 1703, 1626, 1596, 1500, 1461, 1438, 1367; NMR δ_H (400 MHz, $CDCl_3$) 1.41 (9H, s), 2.99 (1H, dd, J = 13.1, 6.8 Hz), 3.12 (1H, dd, J = 13.8, 5.5 Hz), 3.73 (3H, s), 4.56 (1H, dd, J = 13.4, 6.1 Hz), 5.07 (1H, d, J = 7.4 Hz), 6.60−6.75 (3H, m); NMR δ_C (101 MHz, $CDCl_3$) 28.2, 38.1, 52.4, 54.1, 80.2, 102.5 (t, J = 25 Hz), 112.2 (d, J = 13 Hz), 140.0 (t, J = 9 Hz), 155.0, 162.9 (dd, J = 249, 13 Hz), 171.7; $[\alpha]^{22}_D$ +40.4 (c 0.99, $CHCl_3$); MS m/z (ES) found 316.1372, $C_{15}H_{20}NO_4F_2$ requires MH^+ 316.1360.

(*S*)-Methyl 2-(*tert*-Butoxycarbonylamino)-3-(4-(trifluoromethyl)phenyl)propanoate, 4k. Following general cross coupling method A using 4-iodobenzotrifluoride (294 μL, 2 mmol) gave, after purification by silica gel column (5% EtOAc in toluene), **4k** (146 mg, 42%) as a pink/red solid. Method B gave **4k** (147 mg, 42%): mp 78−80 °C; R_f 0.62 (30% EtOAc in toluene); IR ν_{max}(film)/cm^{-1} 2980, 1743, 1703, 1500, 1438, 1367; NMR δ_H (400 MHz, $CDCl_3$) 1.42 (9H, s), 3.09 (1H, dd, J = 13.7, 6.4 Hz), 3.22 (1H, dd, J = 13.6, 5.6 Hz), 3.74 (3H, s), 4.64 (1H, dd, J = 13.7, 6.3 Hz), 5.06 (1H, d, J = 7.7 Hz), 7.27 (2H, d, J = 7.9 Hz), 7.56 (2H, d, J = 8.0 Hz); NMR δ_C (101 MHz, $CDCl_3$) 28.2, 38.3, 52.4, 54.2, 80.2, 125.4, 129.7, 140.3, 155.0, 171.9, two quaternary carbon signals not observed; $[\alpha]^{22}_D$ +28.3 (c 1.06, $CHCl_3$); MS m/z (ES) found 348.1417, $C_{16}H_{21}NO_4F_3$ requires MH^+ 348.1423.

(*S*)-Methyl 2-(*tert*-Butoxycarbonylamino)-3-(3,4-difluorophenyl)propanoate, 4l. Following general cross-coupling, method A using 3,4-difluoroiodobenzene (241 μL, 2 mmol) gave, after purification by silica gel column (5% EtOAc in toluene), **4l** (161 mg, 51%) as a red/brown oil, which solidified on standing. Method B gave **4l** (166 mg, 53%): mp 49−51 °C; R_f 0.59 (30% EtOAc in toluene); IR ν_{max}(film)/cm^{-1} 2978, 2926, 1743, 1700, 1610, 1518, 1436, 1366; NMR δ_H (400 MHz, $CDCl_3$) 1.42 (9H, s), 2.98 (1H, dd, J = 14.1, 6.2 Hz), 3.10 (1H, dd, J = 14.1, 5.4 Hz), 3.73 (3H, s), 4.55 (1H, dd, J = 13.4, 6.0 Hz), 5.02 (1H, d, J = 7.3 Hz), 6.80−6.87 (1H, m), 6.90−6.98 (1H, m), 7.07 (1H, m); NMR δ_C (101 MHz, $CDCl_3$) 28.3, 37.6, 52.4, 54.3, 80.2, 117.2 (d, J = 17 Hz), 118.2 (d, J = 17 Hz), 125.3 (dd, J = 5, 3 Hz), 133.1, 148.6 (dd, J = 58, 13 Hz), 151.1 (dd, J = 58, 13 Hz), 155.0, 171.9; $[\alpha]^{22}_D$ +59.1 (c 1.02, $CHCl_3$); MS m/z (ES) found 316.1369, $C_{15}H_{20}NO_4F_2$ requires MH^+ 316.1360.

(*S*)-Methyl 2-(*tert*-Butoxycarbonylamino)-3-(3-chloro-4-fluorophenyl)propanoate, 4m. Following general cross-coupling, method A using 3 chloro-4-fluoroiodobenzene (255 μL, 2 mmol) gave, after purification by silica gel column (5% EtOAc in toluene)m **4m** (149 mg, 45%) as a red/brown oil, which solidified on standing. Method B gave **4m** (154 mg, 46%): mp 53−55 °C; R_f 0.63 (30% EtOAc in toluene); IR ν_{max}(film)/cm^{-1} 2979, 1743, 1702, 1500, 1437, 1366; NMR δ_H (400 MHz, $CDCl_3$) 1.41 (9H, s), 2.96 (1H, dd, J = 13.9, 6.2 Hz), 3.10 (1H, dd, J = 13.9, 5.5 Hz), 3.72 (3H, s), 4.54 (1H, dd, J = 13.5, 6.1 Hz), 5.04 (1H, d, J = 7.5 Hz), 6.95−7.01 (1H, m), 7.05 (1H, t, J = 8.6 Hz), 7.12−7.20 (1H, m); NMR δ_C (101 MHz, $CDCl_3$) 28.3, 37.4, 52.4, 54.3, 80.2, 116.6 (d, J = 21 Hz), 120.8 (d, J = 17 Hz), 129.0 (d, J = 7 Hz), 131.4, 133.3 (d, J = 4 Hz), 155.0, 157.3 (d, J = 248 Hz), 171.9; $[\alpha]^{22}_D$ +48.5 (c 1.03, $CHCl_3$); MS m/z (ES) found 332.1057, $C_{15}H_{20}NO_4ClF$ requires MH^+ 332.1065.

■ ASSOCIATED CONTENT

Supporting Information. Details of calculated coordinates of all reported structures; additional figure S1; ESI-MS spectrum of the TMEDA cation **3**; assignment of peaks to individual stretching modes in the calculated spectra for cation **3**, with axial (Table 5) and equatorial (Table 6) ester groups. Comparison of NMR chemical shift for the diastereotopic protons of new substituted phenylalanine derivatives (Table 7), tabulated specific rotations for new phenylalanine derivatives in $CHCl_3$ (Table 8), experimental for known compounds, and ^{1}H and ^{13}C NMR spectra for compounds **4g**−**i**,**k**−**m** and **5**. This information is available free of charge via the Internet at http://pubs.acs.org.

■ AUTHOR INFORMATION

Corresponding Author
*E-mail: r.f.w.jackson@sheffield.ac.uk.

■ ACKNOWLEDGMENT

M.S. and F.D. thank Dr. Britta Redlich (FOM Institute) for assistance and the German Science Foundation (DFG) and the European Community for funding (FP7/2007-2013; grant no. 226716). We also thank the EPSRC for a DTA studentship (A.J.R.), Umicore for supplying nano zinc (Nozip), and Professor B. H. Lipshutz for helpful advice.

■ REFERENCES

(1) Dreiocker, F.; Oomens, J.; Meijer, A. J. H. M.; Pickup, B. T.; Jackson, R. F. W.; Schäfer, M. *J. Org. Chem.* **2010**, *75*, 1203–1213.
(2) Polfer, N. C.; Oomens, J. *Mass Spectrom. Rev.* **2009**, *28*, 468–494.
(3) MacAleese, L.; Maitre, P. *Mass Spectrom. Rev.* **2007**, *26*, 583–605.
(4) Fleckenstein, J. E.; Koszinowski, K. *Chem.—Eur. J.* **2009**, *15*, 12745–12753.
(5) Koszinowski, K.; Böhrer, P. *Organometallics* **2009**, *28*, 771–779.
(6) Koszinowski, K.; Böhrer, P. *Organometallics* **2009**, *28*, 100–110.
(7) Di Marco, V. B.; Bombi, G. G. *Mass Spectrom. Rev.* **2006**, *25*, 347–379.
(8) Caggiano, L.; Jackson, R. F. W.; Meijer, A.; Pickup, B. T.; Wilkinson, K. A. *Chem.—Eur. J.* **2008**, *14*, 8798–8802.
(9) Krasovskiy, A.; Duplais, C.; Lipshutz, B. H. *J. Am. Chem. Soc.* **2009**, *131*, 15592–15593.
(10) Duplais, C.; Krasovskiy, A.; Wattenberg, A.; Lipshutz, B. H. *Chem. Commun* **2010**, *46*, 562–564.
(11) Lipshutz, B. H.; Abela, A. R.; Boskovic, Z. V.; Nishikata, T.; Duplais, C.; Krasovskiy, A. *Top. Catal.* **2010**, *53*, 985–990.
(12) Rilatt, I.; Caggiano, L.; Jackson, R. F. W. *Synlett* **2005**, 2701–2719.
(13) Ross, A. J.; Lang, H. L.; Jackson, R. F. W. *J. Org. Chem.* **2010**, *75*, 245–248.
(14) Chalker, J. M.; Wood, C. S. C.; Davis, B. G. *J. Am. Chem. Soc.* **2009**, *131*, 16346–16347.
(15) Boys, S. F.; Bernardi, F. *Mol. Phys.* **1970**, *19*, 553–566.
(16) Irikura, K. K.; Johnson, R. D.; Kacker, R. N. *J. Phys. Chem. A* **2005**, *109*, 8430–8437.
(17) Foresman, J. B.; Frisch, A. E. *Exploring Chemistry with Electronic Structure Methods*, 2nd ed.; Gaussian, Inc.: Pittsburgh, PA, 1996.
(18) Bythell, B. J.; Dain, R. P.; Curtice, S. S.; Oomens, J.; Steill, J. D.; Groenewold, G. S.; Paizs, B.; Van, S. M. J. *J. Phys. Chem. A* **2010**, *114*, 5076–5082.

(19) Lemaire, J.; Boissel, P.; Heninger, M.; Mauclaire, G.; Bellec, G.; Mestdagh, H.; Simon, A.; Le, C. S.; Ortega, J. M.; Glotin, F.; Maitre, P. *Phys. Rev. Lett.* **2002**, *89*, 273002/1–273002/4.
(20) Drayss, M. K.; Blunk, D.; Oomens, J.; Gao, B.; Wyttenbach, T.; Bowers, M. T.; Schäfer, M. *J. Phys. Chem. A* **2009**, *113*, 9543–9550.
(21) Asmis, K. R.; Pivonka, N. L.; Santambrogio, G.; Brummer, M.; Kaposta, C.; Neumark, D. M.; Woste, L. *Science* **2003**, *299*, 1375–7.
(22) Oomens, J.; Tielens, A. G. G. M.; Sartakov, B. G.; von, H. G.; Meijer, G. *Astrophys. J.* **2003**, *591*, 968–985.
(23) Polfer, N. C.; Oomens, J.; Moore, D. T.; Von, H. G.; Meijer, G.; Dunbar, R. C. *J. Am. Chem. Soc.* **2006**, *128*, 517–525.
(24) Frisch, M. J.; Trucks, G. W.; Schlegel, H. B.; Scuseria, G. E.; Robb, M. A.; Cheeseman, J. R.; Scalmani, G.; Barone, V.; Mennucci, B.; Petersson, G. A.; Nakatsuji, H.; Caricato, M.; Li, X.; Hratchian, H. P.; Izmaylov, A. F.; Bloino, J.; Zheng, G.; Sonnenberg, J. L.; Hada, M.; Ehara, M.; Toyota, K.; Fukuda, R.; Hasegawa, J.; Ishida, M.; Nakajima, T.; Honda, Y.; Kitao, O.; Nakai, H.; Vreven, T.; Montgomery, J., J. A.; Peralta, J. E.; Ogliaro, F.; Bearpark, M.; Heyd, J. J.; Brothers, E.; Kudin, K. N.; Staroverov, V. N.; Kobayashi, R.; Normand, J.; Raghavachari, K.; Rendell, A.; Burant, J. C.; Iyengar, S. S.; Tomasi, J.; Cossi, M.; Rega, N.; Millam, N. J.; Klene, M.; Knox, J. E.; Cross, J. B.; Bakken, V.; Adamo, C.; Jaramillo, J.; Gomperts, R.; Stratmann, R. E.; Yazyev, O.; Austin, A. J.; Cammi, R.; Pomelli, C.; Ochterski, J. W.; Martin, R. L.; Morokuma, K.; Zakrzewski, V. G.; Voth, G. A.; Salvador, P.; Dannenberg, J. J.; Dapprich, S.; Daniels, A. D.; Farkas, Ö.; Foresman, J. B.; Ortiz, J. V.; Cioslowski, J.; Fox, D. J. Gaussian, Inc.: Wallingford, CT, 2009.
(25) Jackson, R. F. W.; Moore, R. J.; Dexter, C. S.; Elliot, J.; Mowbray, C. E. *J. Org. Chem.* **1998**, *63*, 7875–7884.
(26) Bordwell, F. G. *Acc. Chem. Res.* **1988**, *21*, 456–463.
(27) Jackson, R. F. W.; Rilatt, I.; Murray, P. J. *Org. Biomol. Chem.* **2003**, *2*, 110–113.
(28) Oepts, D.; Vandermeer, A. F. G.; Vanamersfoort, P. W. *Infrared Phys. Technol.* **1995**, *36*, 297–308.
(29) Polfer, N. C.; Oomens, J. *Phys. Chem. Chem. Phys.* **2007**, *9*, 3804–3817.
(30) Valle, J. J.; Eyler, J. R.; Oomens, J.; Moore, D. T.; van der Meer, A. F. G.; von Helden, G.; Meijer, G.; Hendrickson, C. L.; Marshall, A. G.; Blakney, G. T. *Rev. Sci. Instrum.* **2005**, *76*, 023103.
(31) Becke, A. D. *J. Chem. Phys.* **1993**, *98*, 5648–5652.
(32) Nicklass, A.; Dolg, M.; Stoll, H.; Preuss, H. *J. Chem. Phys.* **1995**, *102*, 8942–8952.
(33) Cao, X. Y.; Dolg, M. *J. Chem. Phys.* **2001**, *115*, 7348–7355.
(34) Tomasi, J.; Mennucci, B.; Cammi, R. *Chem. Rev.* **2005**, *105*, 2999–3093.